Source signature estimation – attenuation of the sea-bottom reflection error from near-field measurements

Ed Kragh, Robert Laws & Ali Özbek

Introduction

Knowing the far-field signature (pulse shape) of a marine seismic source array allows deconvolution of the shot-to-shot variations of the signature, improving consistency of data quality. With the increasing need for higher quality data, suitable for high resolution reservoir monitoring and time-lapse imaging, source-signature deconvolution becomes a requirement.

One method of estimating the far-field signature is the Notional Source Method (Ziolkowski *et al*. 1982; Parkes *et al*. 1984). The method requires near-field recordings to be made close to each airgun, or airgun cluster. In areas where the sea-bottom is either hard or shallow the reflection from the sea-bottom (and trailing seismogram) can be sufficiently high in amplitude in the near-field signatures to cause an error in the far-field signature estimate. Although previously recognized as a possible source of error (Ziolkowski & Johnston 1997), a correction was not thought necessary for the estimation of accurate source signatures. However, we have observed a number of data sets where the sea-bottom reflection error requires correcting.

To a good approximation, the sea-bottom reflection is invariant across the airgun strings, whereas the bubble energy from each airgun differs significantly across each airgun string. This is because the hydrophones lie in the same horizontal plane. The problem lends itself naturally to beamforming techniques, the most simple being either a straight mean or median stack of the near-field recordings.

We found that simple stacking methods do not give sufficient suppression of the bubble energy to allow a good estimation of the contaminating sea-bottom reflection. Instead, we used a linearly constrained adaptive beamformer called LACONA (Özbek 2000). It is applied to each airgun string to give an estimate of the sea-bottom reflection. This estimate is then subtracted from the near-field measurements and then the far-field estimation performed in the usual manner using the Notional Source Method. Suppressing the water-bottom reflection from the near-field measurements prior to estimation of the far-field signature, means that the full directivity of the estimated far-field signature should be corrected.

Discussion of the relative merits of the Notional Source Method compared to other methods of estimating the far-field signature are not presented in this article, the reader is referred Laws *et al*. (1998) for such a discussion. For further details of the method itself the reader is referred to Ziolkowski *et al*. (1982) and Parkes *et al*. (1984). The Notional Source Method is proprietary to Schlumberger and is implemented in the TRISOR[1] digital airgun control system.

Real data example of the sea-bottom reflection error

Figure 1 shows typical near-field measurements from a three-string source array. There are six near-field measurements in each string, one from each airgun or airgun cluster. In this example the airgun volumes are similar on strings one and three, and slightly larger on the second central string. This is reflected in the bubble amplitudes and periods within each string. The low amplitude arrival at about 190 ms (90 ms after the initial peaks) on each near-field is the contaminating reflection from the sea-bottom. This two-way travel time puts the water depth at about 70 m in this example.

The sea-bottom reflection contamination may look small, possibly even insignificant, on the near-fields in Fig. 1. However, because of the summing of the 18 airgun signatures that go into the far-field estimation, the sea-bottom signal coherently stacks to be a significant event on the far-field estimation.

Figure 2 shows the far-field estimation and its spectrum. The lower trace on the left panel is a zoom display (vertical direction only) of the later arrival times. The sea-bottom reflection is a noticeable arrival after the initial peak and this causes spectral ripple with an amplitude of around $\pm$ 1dB. This is undesirable. For example, picking attributes such as the commonly used peak-to-bubble ratio will pick the peak-to-sea-bottom reflection in this case. The first and second order sea-bottom multiples are also visible on the far-field estimation (Fig. 2), and the higher frequency low amplitude jitter arriving after the sea-bottom reflection is due to the trailing seismogram.

Schlumberger Cambridge Research. High Cross, Madingley Road Cambridge, CB3 OEL, UK
Correspondence: Ed Kragh, Schlumberger Cambridge Research.

Sea-bottom reflection attenuation

A linearly constrained adaptive beamformer (LACONA) is applied to each airgun string to give an estimate of the sea-bottom reflection. This estimate is then subtracted from the near-field measurements and then the far-field estimation performed in the usual manner using the Notional Source Method. LACONA is designed to preserve signals incident from a range of target directions, while suppressing interferences incident from other directions. It can also be thought of as an adaptive f-k filter that is adaptive in those parts of the frequency-wavenumber space that contain the interference, but fixed in the regions of the f-k space that contain the signal to be preserved. In this application of LACONA, the sea-bottom reflection is regarded as the signal, while the bubble energy is considered as the interference that has to be attenuated. No knowledge of the 'noise' to be removed (the airgun bubbles in this case) is required.

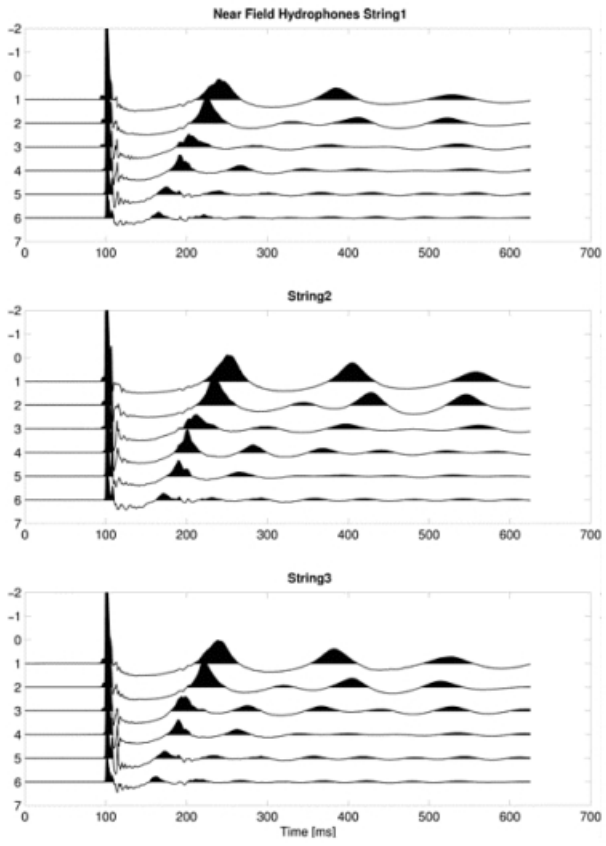

Figure 1 Real data example near-field hydrophone traces from a typical three-string, 18-airgun array, showing sea-bottom reflection contamination. The sea-bottom reflection is the low amplitude arrival at about 190 ms.

Figure 3 shows the far-field signatures estimated from the corrected near-field measurements (plotted in red), with the uncorrected far-field estimate, as shown in Fig. 2, for comparison (plotted in black). There is a clear improvement by attenuation of the sea-bottom reflection, and the corresponding amplitude spectra shows improved smoother character. The remaining ripple in the lower frequencies is due to the residual bubble energy which is then the largest arrival after the initial peak. The peak-to-bubble ratio, for example, would now be estimated correctly. The sea-bottom multiples and trailing seismogram all appear to be corrected from the far-field estimate.

Modelling

The results plotted in Fig. 3 show a clear attenuation of the unwanted sea-bottom reflection. However, there is some residual error. This is due to a combination of error in the sea-bottom reflection estimate; residual bubble energy leaking through the filter, and either distortion or noise introduced by application of the beamformer.

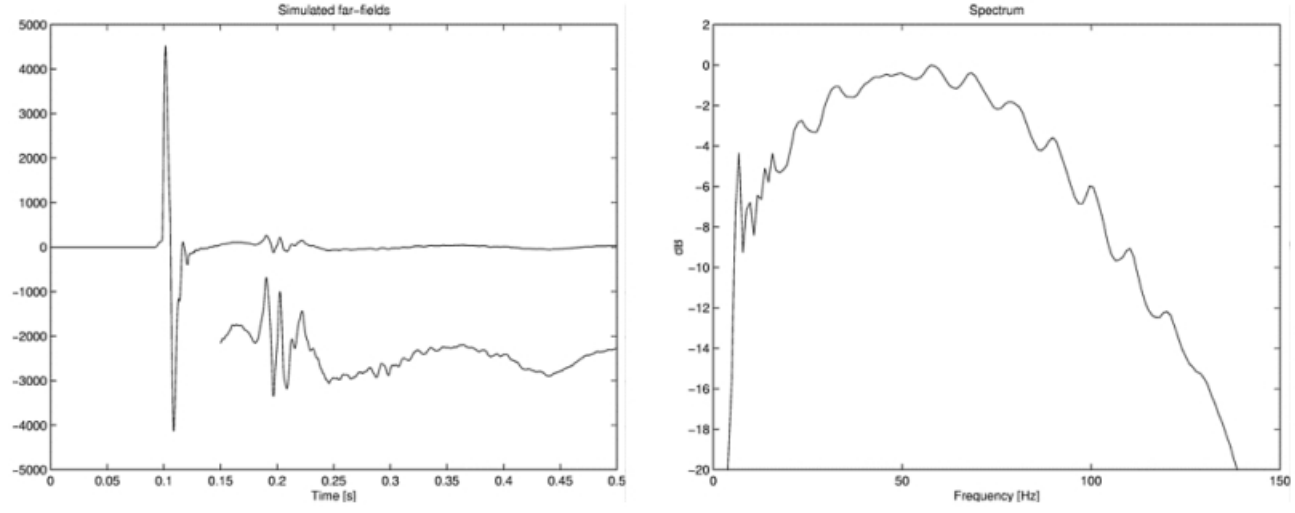

Figure 2 Estimated far-field signature from the near-fields in Figure 1 showing a significant sea-bottom reflection at 190 ms. The lower trace on the left panel is a zoom display (vertical direction only) of the later arrival times. The corresponding amplitude spectrum is shown on the right. There is a spectral ripple of about $\pm$ 1dB in amplitude.

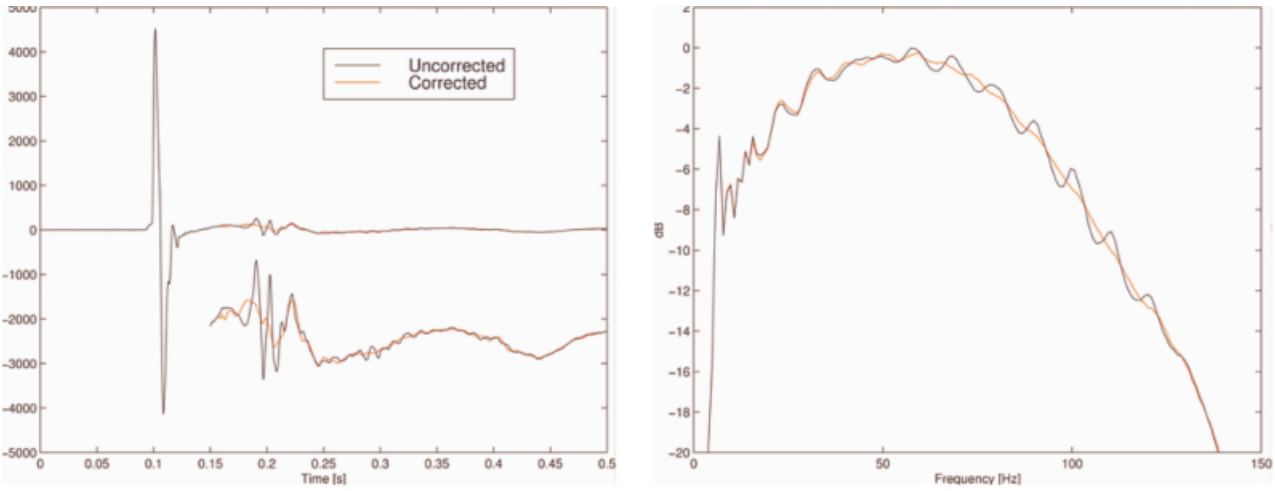

Figure 3 Estimated far-field signatures from uncorrected (as shown in Figure 2) and corrected near-fields for the real data example (Figure 1). The lower trace on the left panel is a zoom display (vertical direction only) of the later arrival times. The corresponding amplitude spectra are shown on the right, and show improved spectral smoothness of the corrected result.

To quantify the effectiveness of the method we carried out some modelling, and in order to keep the modelling realistic (while retaining full control) we used a set of real near-field hydrophone measurements as the raw data. These were acquired in the North Sea using a fairly typical three-string airgun array of 18 near-field measurements. The sea-bottom was at 200–300 m depth and contamination by the reflection negligible. From this set of near-field measurements, a far-field signature was estimated using the Notional Source Method, and this represents the ideal unperturbed result.

The near-field measurements are then corrupted with a synthetic sea-bottom reflection. This is computed as follows: The 'ideal' far-field estimate is scaled in amplitude and delayed in time according to the simulated water depth. The result is then ghosted, representing the reflection from the sea surface with the hydrophones at 5 m depth. A further scaling (less than unity) can be applied to represent the reflection coefficient at the sea bottom. The resulting synthetic sea-bottom reflection is added to the near-field hydrophone traces to give perturbed data (contaminated with a sea-bottom reflection at a chosen depth).

Figure 4 shows the near-field hydrophone traces with a synthetic sea-bottom reflection added. The simulated depth is 100 m and the sea-bottom reflection coefficient is unity.

We processed these perturbed near-field data using the described method. This result is compared to the ideal unperturbed far-field to obtain estimates of the residual error. Figure 5 shows a comparison of the far-field estimates. The raw ideal signature is plotted as a solid black line. The uncorrected signature with the modelled sea-bottom reflection is plotted as a blue dotted line. The corrected signature is plotted as a solid red line. If the correction were perfect, then the corrected signature (red) would match the ideal signature

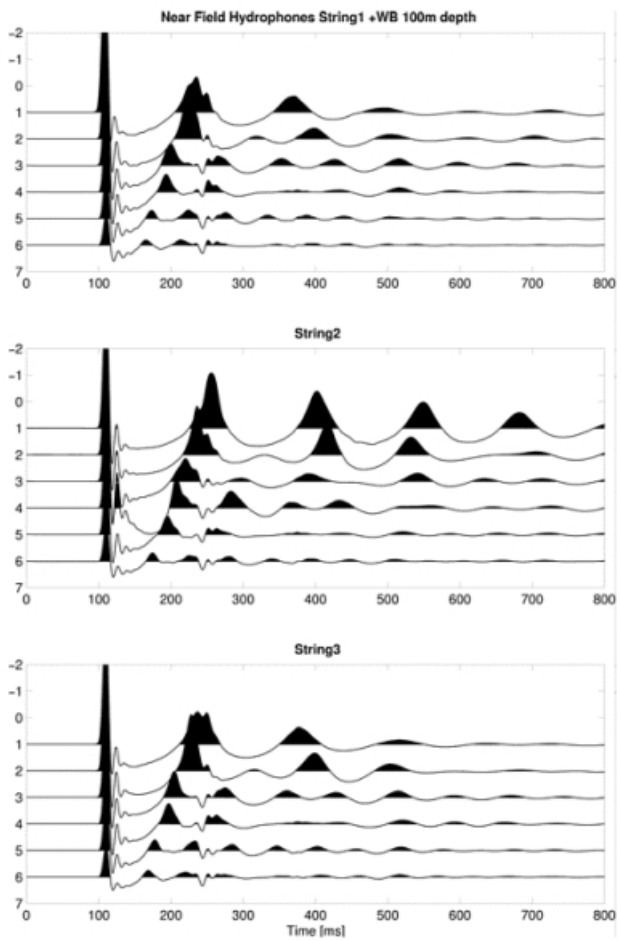

Figure 4 Near-fields with a synthetic sea-bottom reflection added to a simulated water depth of 100 m. These data are used to quantify the effectiveness of the proposed sea-bottom attenuation method.

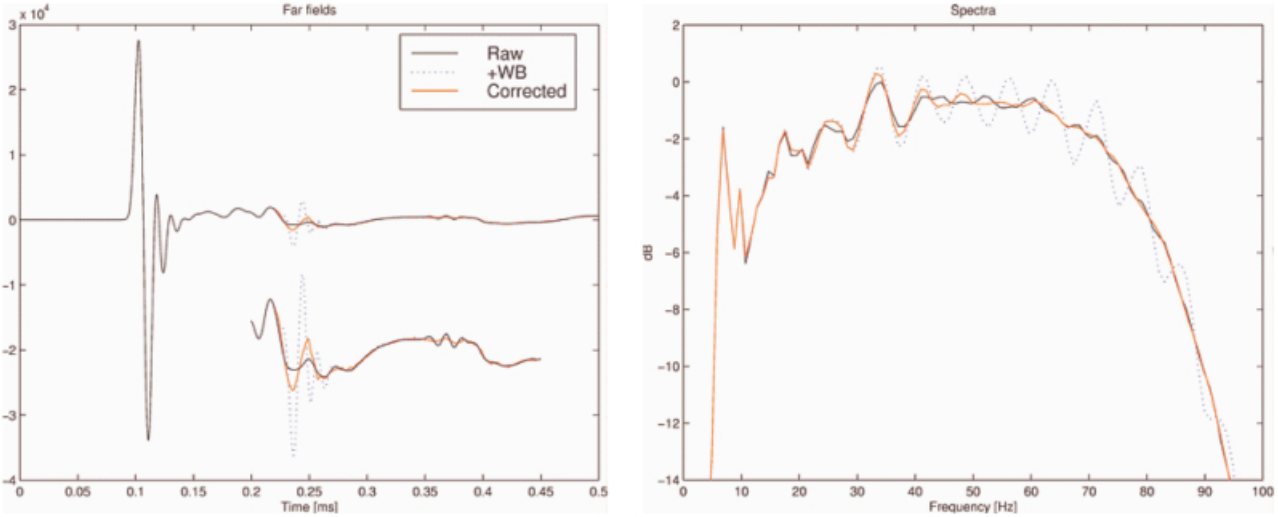

Figure 5 Estimated far-field signatures from uncorrected (Figure 4) and corrected near-fields, using a synthetic sea-bottom reflection appropriate to 100 m depth. The corresponding amplitude spectra are shown on the right. The corrected spectra (which ideally should match the raw spectra) show the residual error to be less than 0.5 dB over the whole bandwidth.

(black). The lower trace in each panel shows the later times plotted with a higher gain.

Although the match is not perfect, it is a clear improvement over the uncorrected signature. The corresponding amplitude spectra are shown on the right, and show the match between the ideal and corrected signatures is to within 0.5 dB over the whole spectrum. We consider this to be an acceptable residual error level. 0.5 dB represents a ~6% amplitude error and is equivalent to a pure phase error of 3.6 degrees.

We observe the (tiny) *real* sea-bottom reflection at about 375 ms on the far-field estimate (Fig. 5), which is not noticeable on the near-fields (Fig. 4). This appears to be attenuated quite successfully, despite its tiny amplitude. For computation of the spectra in Fig. 5, the far-field estimates were windowed such that the tiny real sea-bottom reflection does not affect the spectral computation.

Limitations

The proposed method has two main limitations: Shallow water depth and perturbations of the sea-bottom reflection (the beamformer assumes the reflected signal is identical on all near-field hydrophones).

- The beamformer cannot distinguish a sea-bottom reflection arrival from the direct initial primary pulses from each airgun, or airgun cluster, because these also have zero moveout components across the airgun strings. There is a time after the initial firing before the beamformer can make a clean estimate of the sea-bottom reflection without contamination of the initial airgun pulses. This translates to a minimum depth below which the method is not applicable. Modelling suggests that, as formulated here, the method will work down to water depths as shallow as 40 m which covers many areas where the sea-bottom reflection is problematic.
- Perturbations on the sea-bottom reflection (as measured by the near-field hydrophones) exist for a variety of reasons. For example: airgun-array geometry variations, nonvertical incidence, nonuniform reflection coefficients and nonplanar wavefronts. As a first approximation, these can be represented by amplitude and time perturbations. These perturbations, which compromise the beamformer, can be included in the modelling by adding them to the synthetic water bottom traces. Such modelling indicates that small perturbations can be tolerated with no obvious degradation to the results.

Figure 6 shows a more severe test using the same 'ideal' near-fields. In this case, a sea-bottom depth of 40 m is modelled with a sea-bottom reflection coefficient of 0.4, in order to reduce the amplitude of the contaminating reflection. Further, amplitude and time perturbations are added to the synthetic sea-bottom reflection to test the robustness of the beamformer to perturbations. The amplitude perturbations are 8% RMS and the time perturbations are 1.3 ms RMS, both with coherence lengths of around 100 m. Figure 6 shows that a substantial correction is still achieved for this more severe case. The residual error is within 0.5dB over most of the signal bandwidth.

Conclusion

We have demonstrated a method for attenuating the sea-bottom reflection from near-field hydrophone measurements in order to obtain an improved far-field estimate for the purpose of shot-by-shot deconvolution. A constrained beamformer effectively removes the sea-bottom reflection error from the near-field measurements prior to computation of the far-field estimate using the Notional Source Method.

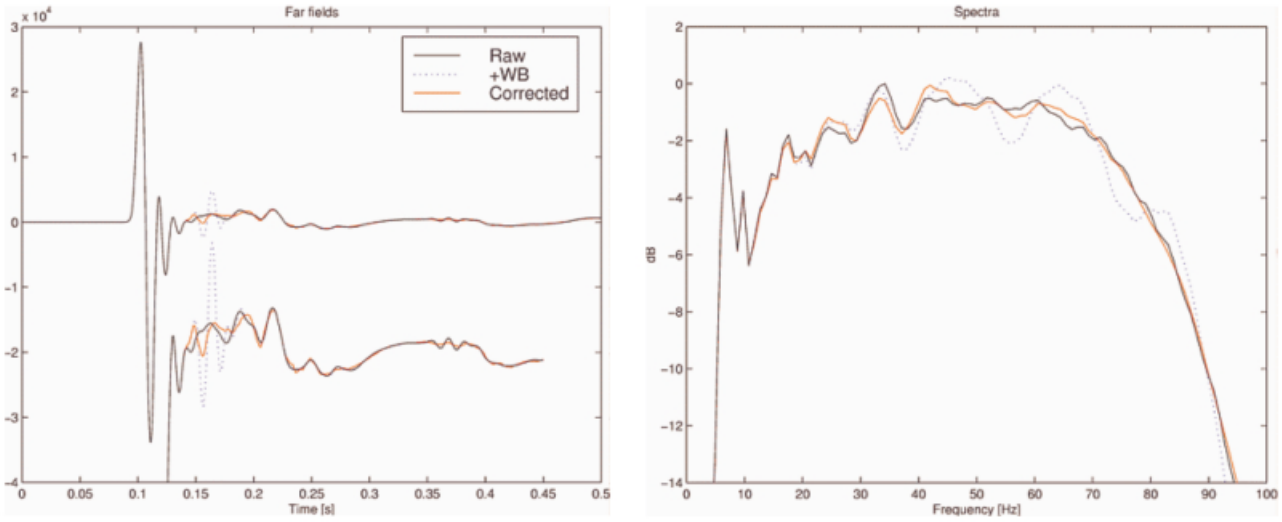

Figure 6 Estimated far-field signatures from uncorrected and corrected near-fields, using a synthetic sea-bottom reflection appropriate to 40 m depth with a sea-bottom reflection coefficient of 0.4. Amplitude (8% RMS) and time (1.3 ms RMS) perturbations are added to the synthetic sea-bottom reflection. The corresponding amplitude spectra are shown on the right. The corrected spectra (which ideally should match the raw spectra) show the residual error to be less than 0.5 dB over most of the bandwidth, even for this more severe case.

Modelling results quantify that the residual error is within 0.5 dB over the whole bandwidth, which is up to around 90 Hz in these examples.

Acknowledgements

We thank Shell UK Exploration and Production for allowing us to show the first real data example, and thank Richard Henman, Håkon Aune and James Martin for discussions and helpful suggestions.

References

Laws, R., Landrø, M. and Amundsen, L. [1998] An experimental comparison of three direct methods of marine source signature estimation. *Geophysical Prospecting* **46**, 353–389.

Özbek, A. [2000] Coherent noise attenuation by adaptive filtering and beamforming. Submitted to EAGE Conference, Glasgow, 2000.

Parkes, G.E., Ziolkowski, A.M., Hatton, L. & Haugland, T. [1984] The signature of an airgun array: computation from near-field measurements including interactions–practical considerations. *Geophysics* **49**, 105–111.

Ziolkowski, A.M. and Johnston, R.G.K. [1997] Marine seismic sources: QC of wavefield computation from near-field pressure measurements. *Geophysical Prospecting* **45**, 611–639.

Ziolkowski, A.M., Parkes, G.E., Hatton, L. and Haugland, T. [1982] The signature of an airgun array: computation from near-field measurements including interactions. *Geophysics* **47**, 1413–1421.

MS submitted November 1999, revised January 2000, accepted February 2000